Hydrodynamic behaviour of micro/nanoscale Poiseuille flow under thermal creep condition

Hassan Akhlaghi, Mojtaba Balaj, and Ehsan Roohi[a)]
High Performance Computing (HPC) Laboratory, Department of Mechanical Engineering, Ferdowsi University of Mashhad, P.O. Box 91775-1111, Mashhad, Iran

(Received 8 June 2013; accepted 26 July 2013; published online 13 August 2013)

Current work investigates the effect of thermal creep on the behavior of rarefied gas flow through micro/nanochannels using the direct simulation Monte Carlo method. Thermal creep effects are studied on velocity profiles, streamwise velocity and pressure, and thermal mass flow rate. The strength of thermal creep is examined at different Knudsen number, channel pressure ratio, and bulk temperature. The thermal mass flow rate variation is investigated over a wide range of flow rarefaction from the slip to free molecular regime. © *2013 AIP Publishing LLC*.
[http://dx.doi.org/10.1063/1.4818678]

The flow between two parallel plates, where a constant unidirectional temperature gradient is applied to the plates, is a common thermal creep flow configuration considered in kinetic approaches. Thermal creep effects move the gas from the cold region towards the hot one. It has different industrial applications such as Knudsen pumps.[1] Even though thermal transpiration effects have been considered by different researchers,[2–6] hydrodynamics behavior of rarefied creeping flow is not considered in detail. As a continuation of our previous work,[7] here we aim to find the thermal creep effects on the hydrodynamic behavior of the Poiseuille flow, i.e., velocity profiles and pressure distribution. Thermal creep effects were produced from a linear wall temperature gradient (WTG) distribution. We also modify our correlated formula for thermal mass flow rate in long micro/nano channels. In this regards, we use an optimized direct simulation Monte Carlo (DSMC)[8] code,[9–13] to perform our simulations.

The geometry of the simulated micro/nanochannel and imposed boundary conditions are shown in Figure 1.

We consider the effect of wall temperature gradient under zero net flow-wall heat transfer condition. To do this, in the first surface cell, we set wall temperature equal to the inflow temperature and keep the average wall temperature equal to the bulk temperature. The effect of different WTG on the centerline pressure distribution through the micro/nanochannel is considered. We applied three different wall temperature gradients of 70 K, 130 K, and 200 K on the channel walls. Figure 2(a) shows that the pressure distribution deviates from the analytical solution as WTG increases. Based on the analytical derivations,[1] the pressure distribution depends on the exit flow average Knudsen number, i.e., the deviation of pressure from the linear distribution increases as the exit average Knudsen number increases. The wall temperature gradient leads to an increase in the exit Knudsen number along the micro/nano channel, see Figure 2(b).

Accordingly, the pressure distribution deviates more with the increase in WTG. In other words, pressure increases through the micro/nano channels as WTG increases. The reason is that the higher wall temperature increases flow compressibility (density variations) more and results in more non-linear pressure distribution. Figure 2(c) shows the pressure deviation from the isothermal condition. Temperature distribution has been also presented in Fig. 2(d). It is inferred from Figs. 2(c) and 2(d) that deviation of pressure and temperature distributions from the isothermal condition is proportional to the magnitude of WTG. In this regards, as the intersection point in the temperature distributions is located in X/L = 1/2, we deduce

$$(T - T_b) \propto \Delta T_w \left(X - \frac{1}{2}\right) \Rightarrow T = T_b + C_1 \Delta T_w \left(X - \frac{1}{2}\right). \tag{1}$$

Similarly, for pressure distribution we could write

$$(P - P_{\Delta T_w = 0}) \propto \Delta T_w \Rightarrow P(x) = P_{\Delta T_w = 0}(x) + C_2(x) \Delta T_w. \tag{2}$$

According to the perfect gas law,

$$\rho = \frac{P}{RT} = \frac{P_{\Delta T_w = 0}(x) + C_2(x) \Delta T_w}{R\left(T_b + C_1 \Delta T_w \left(X - \frac{1}{2}\right)\right)}. \tag{3}$$

Therefore, according to the obtained temperature and pressure distributions, density behavior could also be predicted. Equation (3) shows that there is an intersection point for which density (and consequently Knudsen number) is constant for all

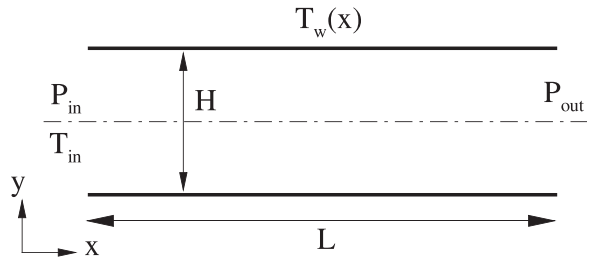

FIG. 1. Micro/nanochannel geometry and imposed boundary conditions.

[a)]Author to whom correspondence should be addressed. Electronic mail: e.roohi@ferdowsi.um.ac.ir. Tel.: +98-511-8805136. Fax: +98-511-8763304.

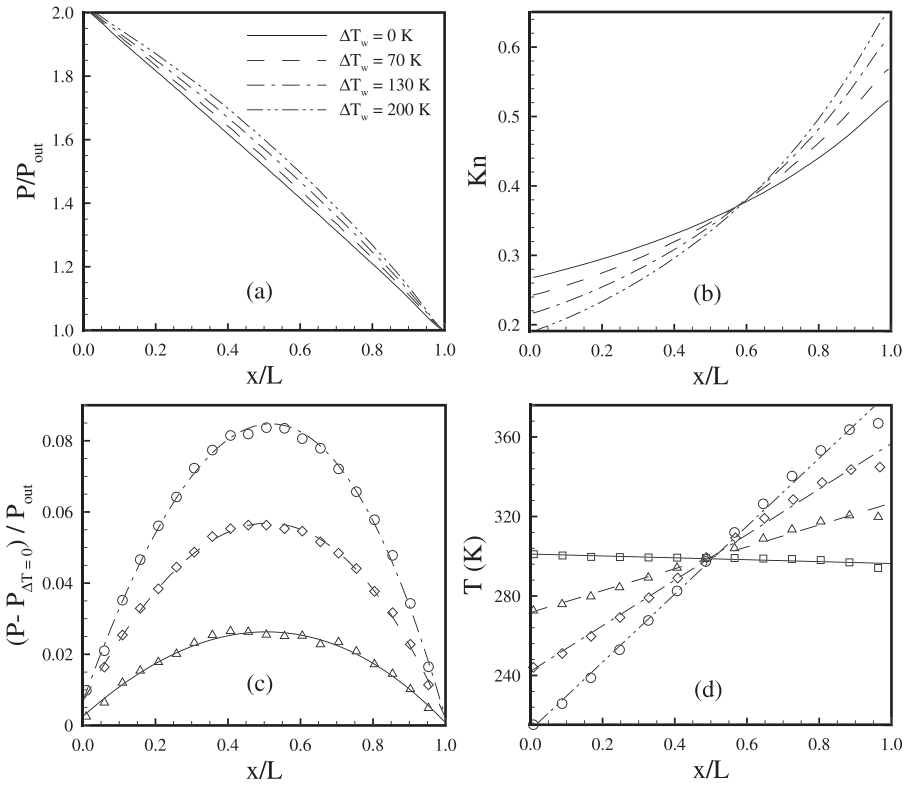

FIG. 2. (a) Pressure, (b) Kn number, (c) pressure difference, and (d) temperature distributions along the micro/nanochannel for different WTG values ($T_b = 300$, pressure ratio $\Pi = 2$, $Kn = 0.4$).

WTG values. The position of intersection point for Knudsen number is obtained from $d(1/\rho)/d(\Delta T_w) = 0$ as follows:

$$T_b C_2(x) - C_1 P_{\Delta T_w = 0}(x)\left(X - \frac{1}{2}\right) = 0. \tag{4}$$

By simulation just one WTG $\neq 0$ case and determination of C_1 and $C_2(x)$, the intersection point for Knudsen number could be specified. According to Eq. (4) and data provided in Figs. 2(c) and 2(d), the location of the intersection point is about $X = 0.58$. This is in good agreement with the intersection point predicted in Fig. 2(b). At the intersection point, from a physical view point, the density and Knudsen number are independent from WTG and are only function of the operational micro/nanochannel condition, i.e., inlet/outlet flow conditions.

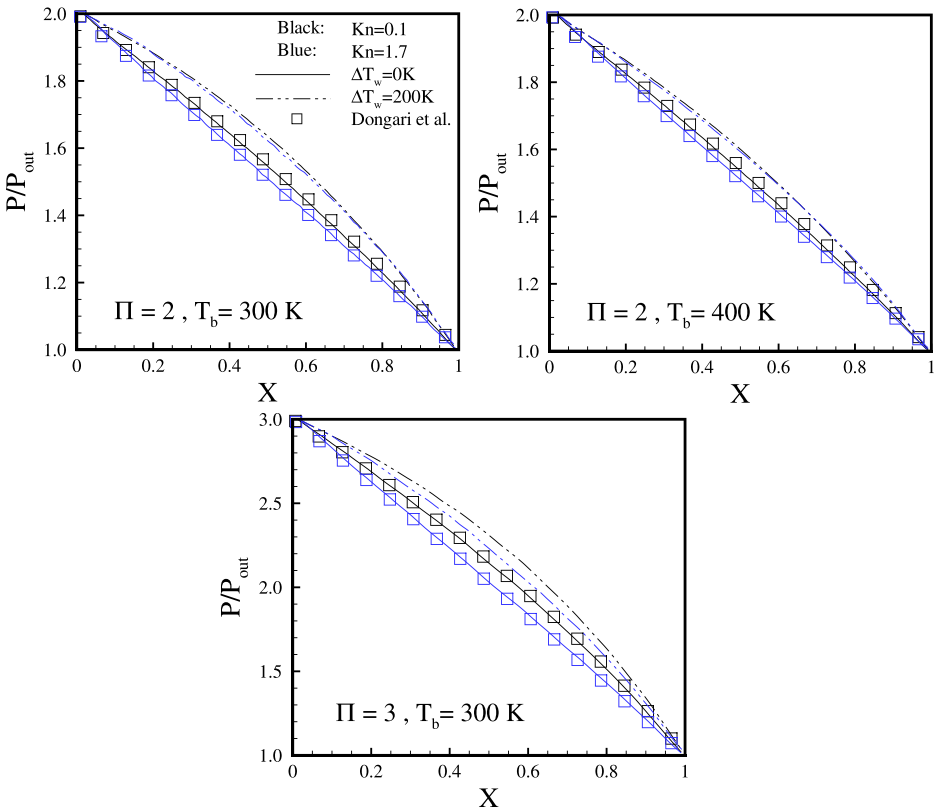

FIG. 3. Effect of WTG on the pressure distribution along the micro/nanochannel.

The effects of different bulk temperature (T_b) and different pressure ratio are studied in Figure 3. Solid and dashed lines correspond to uniform wall temperature distribution ($\Delta T_w = 0$ K) and the case with wall temperature gradient equal to 200 K, respectively. Also, symbols correspond to the analytical solution derived by Dongari *et al.*[14,15] It is well seen that the DSMC results reported with the solid lines are in a good agreement with the analytical solution.

This figure indicates that the difference between uniform wall temperature results and those of WTG $\neq 0$ increases as Knudsen number increases. Moreover, it shows that at the same WTG value, deviation is more for lower bulk temperature. Different pressure ratio solutions under the same bulk temperature show that the deviation is approximately the same for different pressure ratios, i.e., $\Pi = 2$ and $\Pi = 3$.

Studies show that the wall temperature gradient influences on the velocity behavior. This behavior includes dimensional (U) and non-dimensional (U*) velocity profiles and centerline (streamwise) velocity distribution (U_c). Figure 4 illustrates the results for the case under uniform wall temperature (solid line) and the cases with WTG equal to 70, 130, and 200 K.

According to Figures 4(a) and 4(b), higher WTG decreases flow velocity at the inlet section and increases it at the outlet section. Figure 4(c) shows the normalized velocity profiles at a section where Kn = 0.5. This figure shows that WTG (or thermal creep effects) increases the velocity slip under constant Knudsen number. According to Figure 4(d), there is a certain section where centerline velocity remains unchanged against the WTG variation. Since dimensional velocity [Figs. 4(a) and 4(b)] directly depends on the pressure gradient, it is well concluded that WTG decreases the pressure gradient at the first sections of the channel (velocity decrease), while it increases the pressure gradient near the outlet section (velocity increase). This conclusion is consistent with the behavior reported in Fig. 3 for the centerline pressure. The intersection point in Fig. 4(d) could be interpreted similar to our discussion around the intersection point of Fig. 2(b). From the continuity of mass along the channel, for a channel with height H we could write

$$\rho U \propto \Delta T_w,$$
$$\rho U = \frac{\dot{m}_{isothermal}}{H} + C_3 \Delta T_w, \tag{5}$$

where C_3 is a constant which indicates that the mass flow rate increases linearly as WTG increases.[7] From combination of Eqs. (3) and (5), the expression for velocity distribution along the channel could be deduced as a function of WTG as follows:

$$U = \frac{R\left(T_{avg} + C_1 \Delta T_w \left[X - \frac{1}{2}\right]\right)\left(\frac{\dot{m}_{isothermal}}{H} + C_3 \Delta T_w\right)}{\left(P_{\Delta T_w = 0}(x) + C_2(x)\Delta T_w\right)}. \tag{6}$$

The intersection point for velocity profiles could be obtained from $d(U)/d(\Delta T_w) = 0$.

Some test cases are performed to study the effect of average Knudsen number, pressure ratio, and bulk temperature especially on the centerline velocity distribution. Figure 5 compares the results for a case under uniform wall temperature and a case with WTG equal to 200 K. Black, red, and

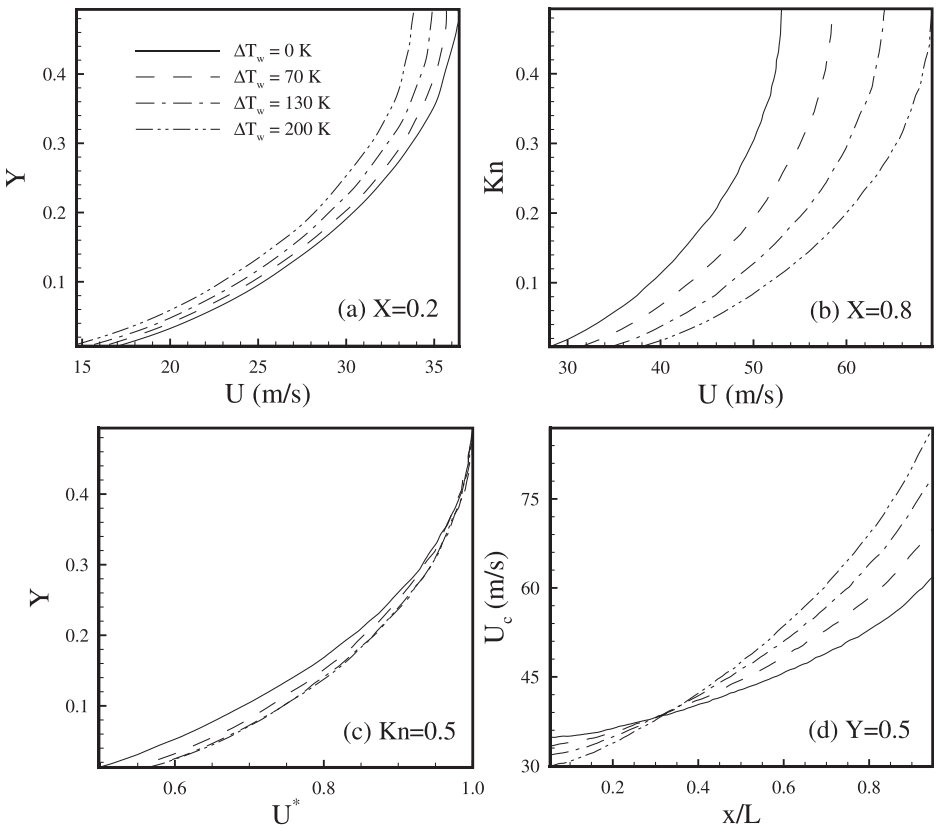

FIG. 4. Effect of WTG on (a) and (b) dimensional and (c) non-dimensional velocity profiles and (d) centerline velocity distribution (T = 300, PR = 2, Kn = 0.4).

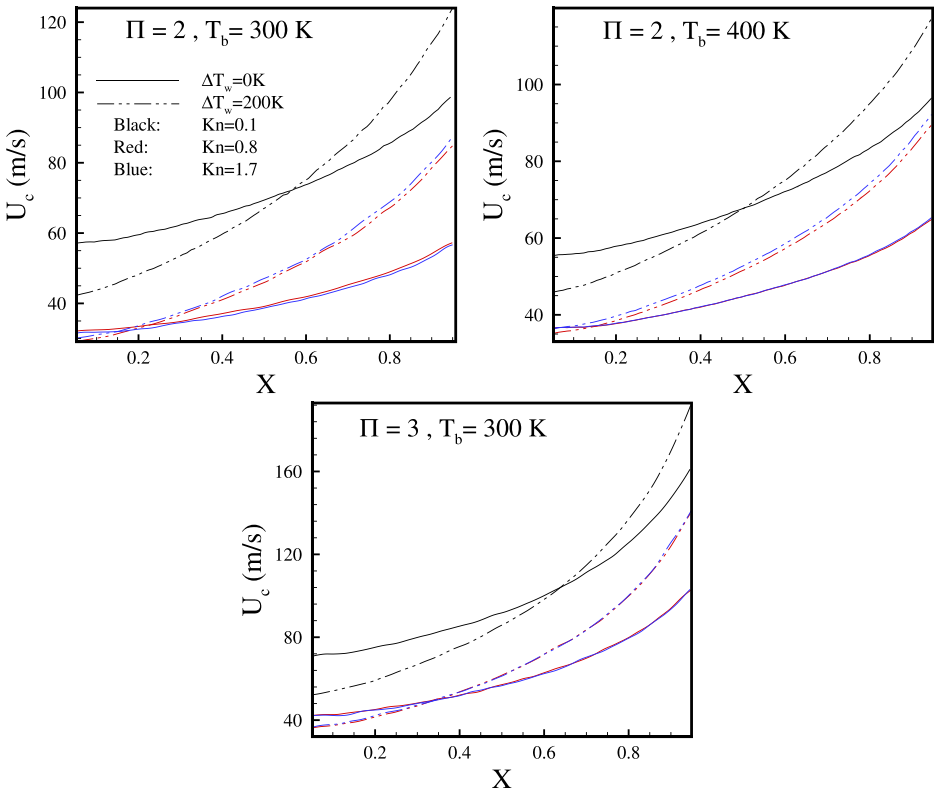

FIG. 5. Effect of WTG on centerline velocity distribution at different micro/nanochannel working conditions and different average flow rarefactions.

blue lines match to "average Knudsen number" equal to 0.1, 0.8, and 1.7, respectively. The effects of WTG are more at lower Π and lower T_b values. Inlet velocity for cases with WTG $\neq 0$ is smaller comparing with that of WTG $= 0$ case. The reason is the lower pressure gradient of the inlet flow for WTG $\neq 0$ case. However, WTG increases pressure gradient such that the outlet velocity is higher for WTG $\neq 0$ cases. Similar to Fig. 4(d), there is an intersection point in which centerline velocities are equal for WTG $= 0$ and WTG $\neq 0$ cases. At higher Kn numbers, the flow acceleration due to WTG effects on the pressure gradient starts at the initial sections of the channel, i.e., $X = 0.2$, while for lower Kn number case of $Kn = 0.1$, this process occurs after the mid-section of the channel, i.e., $X = 0.55$. As T_b increases, the intersection point moves aft, in other words, WTG effects are more pronounced at higher flow bulk temperature. The last frame in Fig. 5 shows the same test case under higher pressure ratio, i.e., $\Pi = 3$. Comparing this frame with the test with $\Pi = 2$ shows that as pressure ratio increases, WTG effects decrease. In other words, WTG is more effective at higher bulk temperature and lower pressure ratio along the channel.

Figure 6 depicts the effect of WTG on the normalized thermal mass flow rate at different working conditions of channel, i.e., different Π, T_b, and average Knudsen number. Thermal mass flow rate is defined as,[7]

$$\dot{m} = \dot{m}_p + \dot{m}_{th}, \tag{7}$$

where subscript "p" corresponds to fully pressure-driven isothermal flow (WTG $= 0$) and subscripts "th" represents thermal mass flow rate due to only WTG $\neq 0$ effects. We call $\dot{m}_p$ and $\dot{m}_{th}$ as pressure and temperature mass flow rate, respectively. Different Kn values of Fig. 6 are created by different levels of inlet/outlet pressure magnitudes.

According to the figure, increase in the thermal mass flow rate due to WTG variations is linear for all levels of flow rarefactions and it is faster for higher Knudsen numbers. The reason is that at higher Knudsen numbers thermal creep effects is stronger. It is well inferred from comparison of solid, dashed, and dashed-dotted lines that thermal creep effect on mass flow rate is stronger at lower Π and T_b values. As it seen, solid lines have the highest slope.

In our previous work,[7] we derived a correlation predicting normalized mass flow rate as a function of Knudsen number.

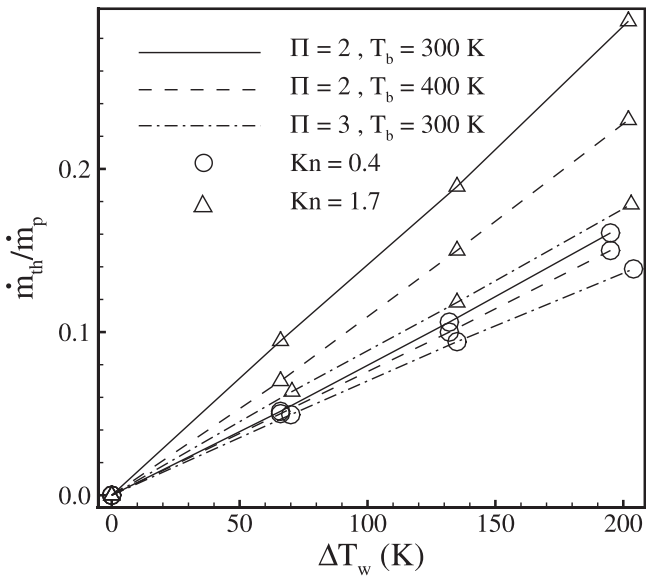

FIG. 6. Normalized thermal mass flow rate as a function of WTG at different working conditions.

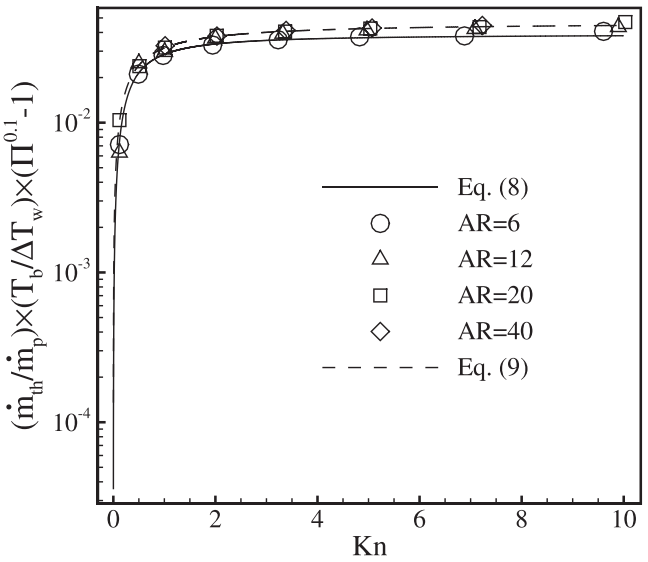

FIG. 7. Normalized thermal mass flow rate versus Kn at different micro/nanochannel AR.

$$\left(\frac{\dot{m}_{th}}{\dot{m}_p}\right) = \left(\frac{0.039Kn^{1.159}}{0.364 + Kn^{1.159}}\right)\left(\frac{\Delta T_w}{T_b}\right)/(\Pi^{0.1} - 1). \quad (8)$$

Equation (8) considers WTG, bulk temperature, channel pressure ratio, and Knudsen number, but it is derived for short channel with aspect ratio (AR) of 6. In the following paragraphs, we extend Eq. (8) for long channels.

One of the most important parameters affecting mass flow rate through micro-/nanochannels is the channel length. We like to emphasize the effect of the channel length on thermal mass flow rate at constant channel height. For this, channel with WTG = 200 K, $\Pi = 2$, and $T_b = 400$ K is considered. Figure 7 shows the normalized thermal mass flow rate as a function of Knudsen numbers for different micro/nanochannel AR (=L/H) values. Solid line is the correlated formula for short micro/nano channels obtained in Ref. 7 and dashed line is the correlated formula of Eq. (9) for long micro/nano channels, which had more practical applications.

$$\left(\frac{\dot{m}_{th}}{\dot{m}_p}\right) = \left(\frac{0.047Kn^{0.95}}{0.49 + Kn^{0.95}}\right)\left(\frac{\Delta T_w}{T_b}\right)\Big/(\Pi^{0.1} - 1). \quad (9)$$

As channel's length increases, both pressure and thermal mass flow rates decrease, but the net results are an increase in the normalized thermal mass flow rate. It can be seen that the results converge to the same line as channel AR increases, i.e., as channel AR increases above 20, the effect of AR becomes negligible.

In conclusion, current work presents hydrodynamic behavior of Poiseuille flow through micro/nanochannels under thermal creep effects. The effects of WTG on the velocity profiles, centerline velocity and pressure, and thermal mass flow rate were investigated. The results detected that an increase in WTG leads to an increase in the pressure distribution's curvature. Velocity profiles at a constant section may increase/decrease as WTG increase due to WTG effects on the pressure distribution gradient. Considering centerline velocity and Kn distributions, there were certain points in which velocity and Kn were independent from WTG. Our study also showed that the WTG effect is stronger at higher flow's bulk temperature and lower channel pressure ratio. Thermal mass flow rate increased linearly with WTG. We present a correlated formula for normalized thermal mass flow rate as a function of the channel's Knudsen number, which is independent from AR of the micro/nano channel.

This work was financially supported by "Iranian Elite Foundation" under Contract No. 100664.

[1]G. E. Karniadakis, A. Beskok, and N. Aluru, *Microflows and Nanoflows: Fundamentals and Simulation* (Springer-Verlag, New York, 2005).
[2]S. K. Loyalka, J. Chem. Phys. **55**, 4497 (1971).
[3]T. Kanki and S. Iuchi, Phys. Fluids **16**, 594 (1973).
[4]T. Ohwada, Y. Sone, and K. Aoki, Phys. Fluids A **12**, 2042 (1989).
[5]A. Alexeenko, S. Gimelshein, E. Muntz, and A. Ketsdever, Int. J. Therm. Sci. **45**, 1045 (2006).
[6]P. Taheri and H. Struchtrup, Physica A **389**, 3069 (2010).
[7]H. Akhlaghi and E. Roohi, *Continuum Mechanics and Thermodynamics* (Springer, 2013).
[8]G. A. Bird, *Molecular Gas Dynamics and the Direct Simulation of Gas Flows* (Oxford Science, Oxford, 1994).
[9]E. Roohi and M. Darbandi, Phys. Fluids **21**, 082001 (2009).
[10]O. Ejtehadi, E. Roohi, and J. A. Abolfazli, Int. Commun. Heat Mass Transfer **39**(3), 439 (2012).
[11]H. Akhlaghi, E. Roohi, and S. K. Stefanov, Int. J. Therm. Sci. **59**, 111 (2012).
[12]A. Mohammadzadeh, E. Roohi, H. Niazmand, S. K. Stefanov, and R. S. Myong, Phys. Rev. E **85**, 056310 (2012).
[13]H. Akhlaghi, M. Balaj, and E. Roohi, Phys. Scr. **88**, 015401 (2013).
[14]N. Dongari, A. Agrawal, and A. Agrawal, Int. J. Heat Mass Transfer **50**, 3411 (2007).
[15]N. Dongari and A. Agrawal, Int. J. Heat Mass Transfer **55**, 4352 (2012).